

RAMAGE, S.J.F.F., PAGALING, E., HAGHI, R.K., DAWSON, L.A., YATES, K., PRABHU, R., HILLIER, S. and DEVALLA, S. 2022. Rapid extraction of high- and low-density microplastics from soil using high-gradient magnetic separation. *Science of the total environment* [online], 831, article 154912. Available from: <https://doi.org/10.1016/j.scitotenv.2022.154912>

Rapid extraction of high- and low-density microplastics from soil using high-gradient magnetic separation.

RAMAGE, S.J.F.F., PAGALING, E., HAGHI, R.K., DAWSON, L.A., YATES, K., PRABHU, R., HILLIER, S. and DEVALLA, S.

2022

This file contains supplementary materials at the end of the main text.

1 **Rapid extraction of high- and low-density microplastics from soil using high-gradient**
2 **magnetic separation**

3 Stuart J. F. F. Ramage^{a,b}, Eulyn Pagaling^a, Reza K. Haghi^a, Lorna A. Dawson^{a,b}, Kyari Yates^b, Radhakrishna
4 Prabhu^b, Stephen Hillier^{a,c}, Sandhya Devalla^a

5 ^a The James Hutton Institute, Craigiebuckler Aberdeen, AB15 8QH, United Kingdom

6 ^b Robert Gordon University, Aberdeen, AB10 7GJ, United Kingdom

7 ^c Department of Soil and Environment, Swedish University of Agricultural Sciences (SLU), SE-75007
8 Uppsala, Sweden

9

10 **ABSTRACT**

11 Microplastics (MPs) are present in all environments, and concerns over their possible detrimental
12 effects on flora and fauna have arisen. Density separation (DS) is commonly used to separate MPs
13 from soils to allow MP quantification; however, it frequently fails to extract high-density MPs
14 sufficiently, resulting in under-estimation of MP abundances. In this proof-of-concept study, a novel
15 three-stage extraction method was developed, involving high-gradient magnetic separation and
16 removal of magnetic soil (Stage 1), magnetic tagging of MPs using surface modified iron nanoparticles
17 (Stage 2), and high-gradient magnetic recovery of surface-modified MPs (Stage 3). The method was
18 optimised for four different soil types (loam, high-carbon loamy sand, sandy loam and high-clay sandy
19 loam) spiked with different MP types (polyethylene, polyethylene terephthalate, and
20 polytetrafluoroethylene) of different particle sizes (63 µm to 2 mm) as well as polyethylene fibres (2-
21 4 mm). The optimised method achieved average recoveries of 96% for fibres and 92% for particles in
22 loam, 91% for fibres and 87% for particles in high-carbon loamy sand, 96% for fibres and 89% for
23 particles in sandy loam, and 97% for fibres and 94% for particles in high-clay sandy loam. These were
24 significantly higher than recoveries achieved by DS, particularly for fibres and high-density MPs ($p <$

25 0.05). To demonstrate the practical application of the HGMS method, it was applied to a farm soil
26 sample, and high-density MP particles were only recovered by HGMS. Furthermore, this study showed
27 that HGMS can recover fibre-aggregate complexes. This improved extraction method will provide
28 better estimates of MP quantities in future studies focused on monitoring the prevalence of MPs in
29 soils.

30

31 **Key Words:** Microplastics; Fibres; Soil; HGMS; Rapid extraction; Electromagnetic

32

33 1. INTRODUCTION

34

35 1.1. Microplastic (MP) particles and fibres are emerging contaminants which are ubiquitous in the
36 natural environment, found in all ecological niches including aquatic (Koelmans et al., 2019;
37 Prata et al., 2019a) and terrestrial environments (Bläsing and Amelung, 2018). Consequently,
38 MPs have been found within organisms (e.g. earthworms) (Chae and An, 2018; Prendergast-
39 Miller et al., 2019; Rodríguez-Seijo et al., 2018), where they have the potential to induce
40 adverse effects such as disruption to endocrine systems (de Souza Machado et al., 2018a)
41 and therefore, have been referred to as long-term anthropogenic terrestrial ecosystem
42 stressors (de Souza Machado et al., 2018b). MPs have also been found within the human
43 body, but current literature on the health consequences of this is limited (Prata et al., 2020;
44 Yan et al., 2022).

45

46 1.2. To accurately assess MP contamination, it is important to extract both high- and low-density
47 MPs. This is a complicated task for soils as they are a complex solid matrix, with broad inter-
48 and intra-sample density and particle size ranges (de Souza Machado et al., 2018a).
49 Additionally, soils often contain high concentrations of organic material that form aggregates

50 around MPs making them difficult to extract (Bläsing and Amelung, 2018; Thomas et al., 2020;
51 Zhang and Liu, 2018).

52

53 1.3. There are several methods that can be employed to extract MPs from soil. Methods that do
54 not rely on plastic density include electrostatic separation (Felsing et al., 2018; Enders et al.,
55 2020) and elutriation (Claessens et al., 2013), however, they have mainly been tested on
56 sediments. Electrostatic separation achieved MP recoveries near 100% when applied to
57 sediments (Felsing et al., 2018), however, MP recoveries were significantly reduced when the
58 method was applied to mineral-rich soils (Enders et al., 2020). Moreover, there was great
59 variability in recovery because it was dependent on MP particle size (Enders et al., 2020).
60 Elutriation is extremely effective for MP removal in sediments (Claessens et al., 2013),
61 however, Grause et al. (2022) reported that the method was not effective for MP extraction
62 from soils due to the wider variability in particle size distributions within soils (Grause et al.,
63 2022). The method also requires large amounts of liquid to fill the column which is impractical
64 if solutions of higher density than water are desired. Another technique which involves the
65 circulation of salt solutions through an enclosed system containing soil has proven highly
66 effective at recovering MPs (Liu et al., 2019).

67

68 1.4. Density separation (DS) takes advantage of the difference in density between plastics and soil
69 particles (Zhang et al., 2019), and is a simple method that has become the most common
70 approach for MP extraction from soil. The density range of most plastics is relatively low at
71 0.9-2.3 g/mL, while the density of most soil particles are higher, averaging around 2.6-2.7
72 g/mL (Prata et al., 2020). DS uses high-density salt solutions such as zinc bromide to
73 resuspend soil, allowing MPs to float while soil particles sink (Han et al., 2019; He et al., 2018;
74 Liu et al., 2018; Masura et al., 2015; Scheurer and Bigalke, 2018; Zhang et al., 2018). While

75 this method has high recovery rates for low-density MPs (Han et al., 2019; Liu et al., 2018;
76 Scheurer and Bigalke, 2018; Zhang et al., 2018), high-density MPs, such as
77 polytetrafluoroethylene and polyvinyl chloride, are not easily recovered due to their densities
78 being similar to bulk soil particles (Liu et al., 2018; Zhang et al., 2018). Moreover, DS suffers
79 from co-extraction of organic matter (making enumeration difficult) (Hurley et al., 2018;
80 Prata et al., 2019b; Wang et al., 2018), long sample processing times (Liu et al., 2018; Scheurer
81 and Bigalke, 2018; Zhang et al., 2018), and issues surrounding the salt solutions'
82 environmental toxicity (Thomas et al., 2020). Since high-density MPs represent > 20% of the
83 global plastic demand (Plastics Europe, 2019), it is important to extract these MPs to
84 accurately determine the levels of terrestrial plastic pollution.

85

86 1.5. Grbic et al. (2019) developed an alternative method to extract MPs involving magnetic
87 separation using surface modified iron nanoparticles, extracting both high- and low-density
88 MPs. Their proof-of-concept work involved the surface modification (hydrophobisation) of
89 iron nanoparticles with hexadecyltrimethoxysilane to enable them to bind to MPs in
90 environmental samples which were subsequently extracted using a neodymium magnet.
91 Their work did not include testing the recovery of MPs from a terrestrial soil matrix. Instead,
92 the method was tested using freshwater, seawater and sediment; however, MP recovery in
93 the sediment was lower with this method compared to that achieved through DS (Grbic et
94 al., 2019). Moreover, damage to the MPs due to removal from the magnet was observed. The
95 principle of magnetic separation using iron nanoparticles was further studied by Shi et al.
96 (2022) for MP removal in water samples, though no details of the type of magnetic extraction
97 system were supplied, and particles were removed from a simple water matrix rather than
98 sediment or soil.

99

100 1.6. A technique known as high-gradient magnetic separation (HGMS) has the potential to
101 improve recovery of MPs from soil, and bypass the methodological issues associated with the
102 previous magnetic extraction method (Grbic et al., 2019). HGMS is widely used to separate
103 micro- and nano-scale particles in aqueous suspensions (Alves et al., 2019; Gerber and Birss,
104 1983; Hillier and Hodson, 1997; Mullins, 1977; Rikers et al., 1998; Watson, 1973; Yavuz et al.,
105 2009), and is widely applied to various matrix separation processes including those in the
106 medical (Bhakdi et al., 2010) and mining industries (Chun, 1995; Dahe, 2000; Ignjatović et al.,
107 1995), and for water purification (Yavuz et al., 2006). Soils contain a vast array of minerals
108 that, even if not ordinarily considered magnetic, are rendered magnetic in the HGMS system,
109 and HGMS is often used to separate these ‘paramagnetic’ minerals from soils (Mullins, 1977).
110 It has also been used to remediate soils from heavy metal contamination and radioactive
111 wastes (Ebner et al., 1999; Rikers et al., 1998). HGMS systems typically consist of a column
112 housing magnetically susceptible wires placed in an electromagnetic field. These wires
113 dehomogenise the field, generating steep gradients that vary across the volume of any
114 particles of appropriate size in the vicinity of the wires, thereby producing a net force on the
115 particles. Particles are separated by the competition between magnetic forces on the one
116 hand, and fluid drag or gravitational forces on the other. The use of an electromagnet is a
117 useful component of the system as it allows the strength of the magnetic field to be adjusted
118 for optimal separation of a wide range of particles with varying complexities, sizes and
119 magnetic susceptibilities. The use of an electromagnetic also allows MPs to be subsequently
120 retrieved after extraction without damaging them by avoiding physical contact with the
121 magnetic source.

122

123 1.7. In this proof-of-concept study, a novel alternative method for extracting MPs from soil was
124 developed, which uses the HGMS technique (Hillier and Hodson, 1997) in combination with

125 the use of hydrophobised iron nanoparticles (Grbic et al., 2019) for binding to the surface of
126 MPs to facilitate high-gradient magnetic separation and subsequent recovery. The three-
127 staged method involves: Stage 1 – initial removal of magnetic soil particles; Stage 2 – tagging
128 of MPs with modified iron nanoparticles to render them magnetic; and Stage 3 – recovery of
129 surface modified MPs. In this method, the MPs do not come into direct contact with the
130 magnet, which avoids damage to the MPs as had been observed in the previous permanent
131 magnetic extraction method developed by Grbic et al. (2019). This novel HGMS method
132 recovered both high- and low-density MPs and fibres from soil, and recovered fibres that
133 were partially embedded in soil aggregates. Furthermore, the developed method was less
134 time-consuming, more cost-effective, and avoided the use of environmentally hazardous
135 chemicals.

136

137 **2. MATERIALS & METHODS**

138 **2.1. Soil Sampling and Soil Chemistry**

139 2.1.1. Four soil types were used to test and optimise the method: loam (Forfar, Angus), high-
140 carbon loamy sand (Dunmaglass, Inverness), sandy loam (Boyndie, Aberdeenshire), and
141 high-clay sandy loam (Hartwood, North Lanarkshire). All soils were air dried and sieved
142 to < 2 mm particles. The optimised method was then tested on a farm soil sample from
143 the Glensaugh Farm Research Facility (Laurencekirk, Aberdeenshire). A composite
144 surface sample (0-10 cm) was collected from the farm (20 kg) using an auger from 50
145 locations in a field (1,144 m²), air dried and sieved to < 2 mm particles. Surface samples
146 were collected because they are more likely to contain MPs. The field was used for
147 livestock grazing. Within the field were several plots experimenting with the application
148 of farmyard manure, compost, sludge pellets and inorganic fertiliser. Samples were not
149 collected from these plots, but were taken elsewhere in the field.

150

151 2.1.2. Glassware and metal tools were used throughout to avoid contamination from plastic
152 utensils, with glassware heated in a muffle oven (450 °C) before use (Dris et al., 2018).
153 Soil clay, silt and sand content were determined by laser diffraction (British Standards
154 Institution, 2009) using a Mastersizer 3000 particle analyser with Hydro LV sample
155 dispersion unit (Malvern Panalytical). Total carbon content was determined by an
156 automated Dumas combustion procedure (Pella and Colombo, 1973) using a Flash 2000
157 Elemental Analyser. Soil chemistry data is given in Table 1. Particle size distribution and
158 carbon content analyses were conducted in this study to accurately determine soil types
159 derived from the soil texture triangle. However, simple hand texturing procedures
160 (Arshad et al., 1997) can be used effectively for determination of the likely experimental
161 conditions required for the soil type concerned.

162

163 2.2. High-Gradient Magnetic Separation (HGMS) System

164 2.2.1. The HGMS arrangement was an in-house, custom-built unit, essentially the same as used
165 by Hillier and Hodson (1997). A 35 cm long magnetic steel collector wire (magnetic
166 matrix; 1.6 mm diameter) was housed within glass tubing (2.5 mm i.d. and 40 cm long)
167 and held using a clamp stand within a magnetic field generated with an electromagnet.
168 The magnetic poles were 40 cm long and 3 cm apart to accommodate the glass tube and
169 the magnetic flux density was set by adjusting the applied current from customised
170 constant current power supplies derived from electrophoresis units (Figure 1). The
171 maximum magnetic flux density achievable in this system with this pole gap was 0.53
172 Tesla. Rubber tubing (Nalgene™; 3/4 in i.d. x 25 cm long) was attached to the bottom of
173 the glass tube and a lock-grip clamp was used here to allow the glass tube to be filled
174 with HPLC grade ethanol (Rathburn, UK) and a separate clamp was used to separate the

175 magnetic material from the non-magnetic material. Samples were added to the glass
176 tubing via a glass funnel.

177

178 **2.3. Stage 1: Removal of Magnetic Soil Particles**

179 2.3.1. Four grams of soil were spiked with 30 MP particles or fibres and mixed thoroughly. Each
180 MP type and MP size was tested with each soil type individually, giving a total of 196
181 individual tests. The MPs tested were 63-75, 106-125, 300-355 and 600-710 μm
182 polyethylene (PE) microbeads (Cospheric LLC, USA), 2-4 mm PE fibres, 2.0 x 2.0 x 0.4 mm
183 polyethylene terephthalate (PET) flakes and 650-850 μm polytetrafluoroethylene (PTFE)
184 fragments, which were prepared in the laboratory. Spiking reached a concentration of
185 1% (w/w) or less, which is a similar concentration to those found in the environment (de
186 Souza Machado et al., 2018b). The soil samples were resuspended in 20 mL of ethanol
187 (Figure 2). The magnetic flux densities were adjusted to locate the optimal conditions
188 for magnetic soil particle removal for each soil (Figure 3; 0.29 Tesla for loam, 0.35 Tesla
189 for high-carbon loamy sand, 0.53 Tesla for sandy loam, and 0.16 Tesla for high-clay sandy
190 loam). Each spiked soil sample was introduced to the magnetic field to allow magnetic
191 soil particles to adhere to the collector wire (3 min settling time). The glass tube was
192 agitated to dislodge any loosely adhered MPs from the wire. The non-magnetic fraction
193 (containing the MPs) that had settled past the collector wire was separated from the
194 magnetic material by a lock grip clamp attached to a flexible Nalgene™ tube and retained
195 for Stages 2 and 3. The magnetic field was switched off and the magnetic soil fraction
196 flushed out and discarded. This was repeated a second time. The collector wire was
197 cleaned for Stage 3.

198

199 **2.4. Stage 2: Magnetisation of MPs**

200 2.4.1. Modified iron nanoparticles were prepared according to Grbic et al. (2019). Briefly, 0.16
201 g of iron nanoparticles (25 nm; Sigma-Aldrich) were mixed with 80 mL ethanol and 800
202 μ L hexadecyltrimethoxysilane for 12 h on a Gallenkamp orbital shaker at 140 rev/min.
203 The liquid was then decanted using a magnet to retain the iron nanoparticles at the
204 bottom of the container, and the modified iron nanoparticles were then re-suspended
205 in 20 mL deionised water for storage. Approximately 10 mg of modified iron
206 nanoparticles were added to the non-magnetic soil fraction retained from Stage 1 using
207 a microspatula and incubated at room temperature for 10 min (with frequent stirring by
208 hand with a glass rod) to allow binding of the iron nanoparticles to the MPs (Figure 2).

209

210 2.5. Stage 3: Extraction of Microplastic Particles

211 2.5.1. The magnetic flux densities were adjusted to the optimal conditions for MP recovery for
212 each soil (Figure 3) - 0.39 Tesla for loam, 0.39 Tesla for high-carbon loamy sand, 0.53
213 Tesla for sandy loam, and 0.39 for high-clay sandy loam. The sample was introduced to
214 the HGMS system and the magnetic fraction retained. The process was repeated for a
215 second cycle with the non-magnetic fraction (adding another \sim 10 mg of modified iron
216 nanoparticles). The retained fractions containing MPs were filtered onto 1.2 μ m
217 Whatman GF/C glass microfibre membrane filters (Figure 2).

218

219 2.6. Density Separation (DS)

220 2.6.1. Four grams of the test soils were spiked with MPs and fibres as described above,
221 resuspended in 50 mL of saturated zinc bromide solution (density \approx 2.4 g/mL³) and
222 placed on an IKA® KS 260 basic rotary shaker at 300 rpm for 5 min and allowed to settle
223 overnight. As with the HGMS method, a total of 196 individual spiked soil tests were
224 processed by DS.

225

226 2.6.2. Eight grams of soil from the Glensaugh Research Facility was used directly (i.e. without
227 spiking) and processed in the same way as the test soils prior to extraction. Previously
228 published studies using DS as the extraction method used sample sizes of 5-10 g of soil
229 (Corradini et al., 2019; Radford et al., 2021; Zhang et al., 2018), so the 8 g used in this
230 study aligns with this practice. Moreover, previously published studies tested soils in
231 triplicate (Corradini et al., 2019; Han et al., 2019; Liu et al., 2018; Radford et al., 2021;
232 Scheurer and Bigalke, 2018; Zhang et al., 2018), but for improved statistics, 7 replicates
233 was used in this study.

234

235 2.6.3. Zinc bromide is a common salt solution and was used in this study as it has the potential
236 to extract both high- and low-density MPs (He et al., 2018; Liu et al., 2018; Scheurer and
237 Bigalke, 2018; Zhang et al., 2018). The deionised water used to make the saturated salt
238 solution was filtered before preparation to minimise the possibility of any MP
239 contamination. The solution was decanted and rinsed with excess solution using a glass
240 pasture pipette while carefully inverting the beaker to reduce the potential loss of
241 microplastics through their adhesion to the walls of the beaker. The decanted and rinsed
242 solution was filtered as described above, and the process repeated a second time.

243

244 2.7. Quantification and Identification of Microplastics

245 2.7.1. Recovered material was treated with 10 mL 30% hydrogen peroxide (Sigma-Aldrich) for
246 1 h at 60 °C to remove organic matter from the MPs, and then re-filtered. MPs were
247 counted directly on the filter papers using a Nikon SMZ1500 stereo microscope (10x
248 magnification). Both HGMS-recovered MPs and DS-recovered MPs were quantified from

249 7 replicates per test soil type and MPs extracted from the Glensaugh sample by HGMS
250 and DS were also quantified from 7 replicates. A blank measurement was also performed
251 with all reagents only. Attenuated Total Reflection - Fourier-Transform Infrared (ATR-
252 FTIR) measurements of MPs that were > 70 µm were carried out using a Bruker Vertex
253 70 FTIR spectrometer. To generate an IR spectrum, a Diamond Attenuated Total
254 Reflectance (DATR) crystal with a single reflectance system was used. Data points in the
255 range of 4000-400 cm⁻¹ were recorded with a resolution of 4 cm⁻¹ and an average of 200
256 scans. An air blank spectrum, with the same number of scans and resolution was
257 recorded as the background spectrum before each measurement. Interpretation of the
258 IR spectra was achieved using searchable in-house and commercial libraries of reference
259 IR spectra.

260

261 **2.8. Statistical Analysis**

262 2.8.1.Recovery of MPs was calculated as a percentage of the total number of spiked MPs. T-
263 tests were performed to find the significance associated with the differences in MP
264 recovery between the two methods (Welch, 1938). This is an appropriate statistical test
265 to use when n is as small as 2 and the within-pair correlation is high (> 0.8) (de Winter,
266 2013). ANOVA was performed to find the significance associated with the differences in
267 recovery of each MP particle type and fibres within each soil type for HGMS (Sthle and
268 Wold, 1989). Both tests were performed using R (version i386 4.0.0).

269

270 **3. RESULTS AND DISCUSSION**

271 **3.1. Optimisation of MP recovery using the HGMS system**

272 3.1.1.Stage 1 of the HGMS method was implemented to remove naturally paramagnetic
273 minerals (Mullins, 1977) and prevent them coating the collector wire and blocking

274 adherence of the MPs. Stage 2 magnetically tagged MPs by binding modified iron
275 nanoparticles to their surface. Stage 3 recovered the MPs that were hydrophobically
276 attached to modified iron nanoparticles, which rendered them magnetic in the HGMS
277 system.

278

279 3.1.2. Magnetic flux densities for Stages 1 and 3 were optimised for each soil type (Figure 3).

280 Particle capture in an axial HGMS system, configured as herein, depends on the
281 competition between gravity settling forces and magnetic forces (Watson, 1973), with
282 the latter a function of both the magnetic susceptibility of any given particle (or
283 aggregate) and its radius. This means that polymer type would not affect magnetic
284 recovery using HGMS - this is determined only by particle size and the ability of the
285 modified iron nanoparticles to bind to the MP's surface. Plastics are diamagnetic (Keyser
286 and Jefferts, 1989) and would ordinarily be repelled from the HGMS filter, but tagging
287 with iron nanoparticles effectively renders them paramagnetic in the HGMS system.
288 Grbic et al. (2019) reported that the iron nanoparticles bound to PE, PET, polypropylene,
289 polyvinyl chloride, polystyrene and polyurethane, and this study has further
290 demonstrated that iron nanoparticles also bound to both PTFE particles and PE fibres
291 (Figure 4). The MPs selected in this work encompassed various chemical and physical
292 properties, such as polar (PET) and non-polar (PE and PTFE) plastics, low-density (PE)
293 and high-density (PET and PTFE) plastics, and different shapes (fibres, spheres, flakes,
294 fragments) and sizes (63 μm to 2 mm) to demonstrate the ability of HGMS to extract
295 plastics with different properties without significant reductions in their recovery.

296

297 3.1.3. Shi et al. (2022) reported that the hydrophobicity and crystallinity of MPs affected the
298 adsorption efficiency of the modified iron nanoparticles. The lower the hydrophobicity

299 and crystallinity of the polymer, the lower the adsorption capacity of the iron
300 nanoparticles, however, the polarity and pH of the background solution can influence
301 this. Ethanol molecules are amphiphilic so have hydrophobic and hydrophilic properties.
302 No significant differences in recovery of the plastic types were observed ($p > 0.05$),
303 therefore, it was concluded that these physicochemical properties did not play a
304 significant role in MP recovery in the HGMS system.

305

306 3.1.4. Differences in optimal conditions can be ascribed to factors such as different particle
307 size distributions (Table 1), and differences in mineralogy and carbon content inasmuch
308 as this determines the magnetic susceptibility of the particles or aggregates present.

309

310 3.1.5. Both loam and high-carbon loamy sand had similar relationships between magnetic flux
311 density and MP recovery (Figures 3A and 3B). In Stage 1, magnetic flux densities > 0.35
312 Tesla removed the most magnetic soil material, but this also removed $> 40\%$ of
313 untreated MPs. Studies have reported that MPs bind to the surface of clay particles in
314 soil (Pathan et al., 2020). This may account for the loss of some MPs in Stage 1,
315 particularly for the loam soil (10.07% clay; Table 1), due to paramagnetic clay particles
316 being attracted to the collector wire. Some types of organic matter may also behave
317 paramagnetically and become attracted to the collector wire, and at stronger magnetic
318 flux densities, organic matter behaving diamagnetically may also be attracted to parts
319 of the collector wire (Sokolowska et al., 2016). MPs have been found to adhere to the
320 surface of vegetation/organic matter (Mateos-Cárdenas et al., 2021), therefore, any
321 MPs adhered to the surface of organic matter in the HGMS system has the potential to
322 be removed through para- or diamagnetic attraction of the organic matter to the
323 collector wire in Stage 1, particularly in soils containing a higher organic matter content

324 such as the high-carbon loamy sand (14.4% carbon; Table 1) used in this study. At 0.10-
325 0.35 Tesla, a maximum of only 9% of untreated MPs were removed. Therefore, an
326 appropriate magnetic flux density was selected that allowed maximum removal of
327 magnetic soil material, without causing significant losses of untreated MPs. This was
328 0.29 and 0.35 Tesla for loam and high-carbon loamy sand, respectively.

329

330 3.1.6. High-clay sandy loam displayed a similar pattern of behaviour to loam and high-carbon
331 loamy sand for MP removal in Stage 1, however, the removal of untreated MPs was
332 higher at magnetic flux densities > 0.20 Tesla (Figure 3C). This was expected for this soil
333 type as there was a higher proportion of clay particles (21.00% clay; Table 1) that could
334 adhere to the surface of MPs, and so MPs may have been removed at lower magnetic
335 flux densities due to this clay-MP interaction. Therefore, a suitable magnetic flux density
336 of 0.16 Tesla was selected for high-clay sandy loam.

337

338 3.1.7. By contrast, MP removal from sandy loam during Stage 1 remained constant across the
339 range (Figure 3D) due to its low carbon and clay content, so 0.53 Tesla was selected for
340 this soil type.

341

342 3.1.8. In Stage 3, MP recovery decreased at electromagnetic strengths > 0.4 Tesla for loam,
343 high-carbon loamy sand and high-clay sandy loam soils due to larger volumes of soil
344 particles (that were not removed in Stage 1) adhering to the collector wire, likely
345 because the resultant deposit effectively blocked the attraction of iron-bound MPs.
346 Therefore, to achieve optimum recovery of MPs, a uniform 0.39 Tesla was selected for
347 Stage 3 in the loam, high-carbon loamy sand and high-clay sandy loam soils (Figures 3A-

348 C). For the sandy loam, optimal MP recovery occurred at the highest magnetic flux
349 density (0.53 Tesla; Figure 1D) because most magnetic soil particles were removed
350 during Stage 1.

351

352 3.2. Performance of HGMS method

353 3.2.1. HGMS achieved significantly higher recoveries for both high- and low-density MPs in all
354 the test soil types compared to DS ($p < 0.01$; Figure 4). The exception was recovery of PE
355 (300-355 μm) in high-carbon loamy sand and sandy loam, and PE (600-710 μm) in high-
356 clay sandy loam, which showed no statistical difference between the two methods ($p >$
357 0.05). A global t-test (i.e. a t-test performed on all 392 tests for MP recovery by DS and
358 HGMS) showed that overall, HGMS gave significantly higher MP recoveries than DS ($p <$
359 0.01).

360

361 3.2.2. The average recovery of PE (63-75 μm) was $89 \pm 5\%$ using DS and $98 \pm 2\%$ using HGMS. The
362 recovery of PE (106-125 μm) was $90 \pm 4\%$ using DS and $96 \pm 3\%$ using HGMS. The higher
363 recoveries of these very small MPs achieved by HGMS is important because small MPs
364 have greater detrimental impacts on organisms (Huerta-Lwanga et al., 2016; Ng et al.,
365 2018) so it will allow future studies to consider impacts on soil biota. Moreover, small
366 MPs are usually difficult to handle in the laboratory so they often get missed. Recovery
367 of PE (300-355 μm) was $90 \pm 4\%$ using DS but $94 \pm 4\%$ using HGMS. The recovery of PE
368 (600-710 μm) was $89 \pm 6\%$ using HGMS, but only $75 \pm 7\%$ using DS. PET had a recovery of
369 $56 \pm 7\%$ using DS and $88 \pm 5\%$ using HGMS. A significant improvement in recovery for the
370 highest density polymer tested, PTFE, was observed using HGMS. PTFE was not
371 recovered at all using DS, but recoveries of $90 \pm 5\%$ were achieved with HGMS. DS is often
372 incapable of extracting high-density MPs due to their density being similar to that of soil

373 particles (Scopetani et al., 2020). High-density polymers are manufactured to be
374 resistant to environmental, chemical and thermal degradation. This can be achieved
375 through their polymeric structures (e.g. the high bonding energy of C-F covalent bonds
376 in PTFE (485 kJ/mol) renders the structure chemically inert), or through the addition of
377 additives to improve their functionality. Due to their resistance to degradation in the
378 environment, they will likely accumulate over time. Until recently, there has been a lack
379 of attention to the presence of high-density MPs in the environment despite their low
380 degradability as well as their contribution of more than 20% of the global plastic demand
381 (PlasticsEurope, 2019). Therefore, the recovery of high-density MPs using HGMS is an
382 important aspect as it will allow a more accurate determination of MP prevalence in soil.

383

384 3.2.3.HGMS also showed improved recovery for fibres (95±3%) compared to DS (78±9%).

385 Fibres are one of the most commonly occurring MPs in the environment (Corradini et
386 al., 2019; Henry et al., 2019), therefore, it was important that the HGMS method was
387 capable of extracting fibres.

388

389 3.2.4.Most HGMS recoveries had smaller standard deviations than DS, (the exception was PE
390 (300-355 µm) where they were the same), indicating that HGMS has better
391 reproducibility compared to both DS and to the previous magnetic extraction method
392 developed by Grbic et al. (2019) (±6-47%). There was no significant difference in
393 recovery of small-sized MPs (63-75 µm PE and 2-4 mm PE fibres), medium-sized MPs
394 (106-125 µm PE and 300-355 µm PE) or large-sized MPs (600-710 µm PE, 2.0 x 2.0 x 0.4
395 mm PET and 650-850 µm PTFE) between the replicates in all 4 soil types ($p > 0.05$),
396 indicating that the HGMS method is highly reproducible when extracting fibres and MPs
397 from these soil types. The exception was in the high-carbon loamy sand where there was

398 a significant difference between replicates when recovering the small-sized MPs, likely
399 as a result of their removal in Stage 1 ($p < 0.05$) (Mateos-Cárdenas et al., 2021).

400

401 3.2.5. Background levels of MP particles and fibres in the test soils were determined by HGMS
402 and optical microscopy (at 10x magnification) to allow accurate measurements of MP
403 recovery from the test soils used for both HGMS and DS. Only fibres were detected in all
404 test soils except for the high-carbon loamy sand. No MP particles were detected in the
405 test soils. These contaminant fibres were bright and long so they were easily
406 distinguished from the spiked fibres, and were discounted from the recovery
407 calculations. Blank control measurements showed that no MP particle or fibre
408 contaminants were detected in any of the reagents (zinc bromide or ethanol containing
409 modified iron nanoparticles) after filtration. All glassware was regularly heated in a
410 muffle oven at 450 °C to reduce the potential for MP contamination (Dris et al., 2018).
411 Therefore, we are confident that the difference in recovery rates obtained from HGMS
412 and DS, respectively, were not a result of differences in background levels of MP
413 particles or fibres in the test soils or reagents.

414

415 3.2.6. Taken together, HGMS achieved good MP recoveries irrespective of density, size or
416 shape of the MP under the conditions set using the optimal magnetic flux densities
417 selected for each soil type. However, reproducibility may be compromised for small-
418 sized MPs (63-75 μm PE and 2-4 mm PE fibres) in high-carbon loamy sand. Several
419 studies found high-density MPs to be either low in quantity or absent in soil (Liu et al.,
420 2018; Scheurer and Bigalke, 2018). This may reflect inefficient extraction methods,
421 which subsequently under-estimated the true abundance of high-density MPs.

422 Implementation of the HGMS method in future studies has the potential to provide
423 more accurate quantifications of MPs and fibres.

424

425 3.2.7. The use of an electromagnet prevented fragmentation of MPs. This is an improvement
426 on the previous magnetic extraction method developed by Grbic et al. (2019), which
427 reported fragmentation and damage of MPs during their removal from the permanent
428 magnet, which could result in over-estimation of MP particle abundance in real
429 environmental samples.

430

431 3.3. Practical application of the HGMS method to a farm soil sample

432 3.3.1. The performance of the HGMS method was additionally tested against DS using a sandy
433 loam soil sample from the Glensaugh Farm Research Facility (Table 1). Agricultural soils
434 have been identified as being a major 'hot-spot' for MP pollution due to land
435 management practices such as sewage sludge amendment and the use of mulching film
436 (Guo et al, 2020). Seven replicates of 8 g of soil were used for analysis, with the sample
437 being split into two 4 g subsamples for HGMS. The magnetic flux densities selected were
438 based on the parameters prescribed to the test soil types. The main factors considered
439 in determining the magnetic flux densities for Stages 1 and 3 were the clay and carbon
440 content. Since the rate of MP recovery was sensitive to these soil factors (Section 3.1),
441 and the Glensaugh sample contained a higher carbon content (Table 1), weaker
442 magnetic flux densities were used compared to the sandy loam test soil. Based on these
443 factors, 0.35 and 0.39 Tesla for Stage 1 and 3, respectively, were selected for the
444 Glensaugh sample and the extraction was carried out as described (Section 2.3-2.6;
445 Figure 2). HGMS extracted an average of 14 ± 4 fibres and 3 ± 1 MP particles per 8 g sample
446 while DS recovered an average of 8 ± 3 fibres and 1 ± 1 MP particle (Figure 5). Particles

447 were predominantly film fragments (potentially originating from the use of silage and
448 haylage plastic wrapping) with the other particles being fragments and flakes. Fibres and
449 MP particles may also have originated from MP pollution that drifted onto the field by
450 wind transportation from nearby experimental soil amendment plots which are known
451 to contain MPs (Corradini et al., 2019; Gui et al., 2021; Rolsky et al, 2020; Vithanage et
452 al., 2021).

453

454 3.3.2. The within-pair correlation between the MP recoveries with HGMS and DS was high (>
455 0.8), which meant that Welch's t-test was an appropriate test to use when looking for
456 significant differences in recoveries. This showed that there was a significant difference
457 in MP recovery between the two methods ($p < 0.05$), likely due to MPs becoming
458 trapped by settling soil aggregates, reducing extraction efficiency during DS (Zhang and
459 Liu, 2018). Fibres recovered from the Glensaugh sample ranged from approximately 2
460 to 15 mm in length, while the dimensions of the particles ranged from approximately 90
461 to 450 μm , and the PE films were an average of approximately 3 x 1.5 x 0.1 mm. The MP
462 particles and fibres recovered were of a different size, colour, and shape to those used
463 during the method development stage, ruling out any possibility of cross-contamination.
464 Fibres that were partially entrapped in soil aggregates were successfully recovered using
465 HGMS (Figure S1), possibly due to the combined effects of the bound iron nanoparticles
466 to the fibre's surface and the magnetically susceptible soil minerals within the
467 aggregate. No such observation was seen with DS. DS often fails to extract fibres or MP
468 particles entrapped within aggregates (Bläsing and Amelung, 2018) due to their overall
469 higher density. Disaggregation steps such as ultrasonication can be undertaken to
470 improve MP recovery during DS, however, the extent of ultrasonication is dependent on
471 soil type and the aggregate's stability, and care must be taken to minimise further

472 interference of the flotation of low-density soil organic matter caused during
473 disaggregation (Thomas et al., 2020). Ultrasonication also has the potential to damage
474 or fragment MPs. This means that the developed HGMS method has the potential to
475 offer extraction of these commonly observed fibre-aggregate complexes resulting in
476 higher recoveries and a more accurate quantification of terrestrial fibre and MP
477 pollution.

478

479 3.3.3.ATR-FTIR was used to confirm the compositions of the MPs recovered from the
480 Glensaugh soil samples (Figure 6), where MP particles were $\geq 70 \mu\text{m}$. As a control, FTIR
481 analysis was also performed on the pristine MPs (selected from the stock containers)
482 used to spike the soils. This was done to ensure the presence of the bound modified iron
483 nanoparticles on subsequently recovered MPs did not interfere with FTIR measurements
484 (Figure S2 and 6). Spectral interpretation identified predominantly PE, PET-glycol and
485 polyester, or blends of these plastic types for recovered fibres, PE for film fragments,
486 and PE and PTFE for particles (Figure 6). This demonstrated that other plastic types could
487 be recovered using HGMS other than those tested during the method optimisation stage
488 of this work. FTIR also confirmed that HGMS recovered both high- and low-density MPs.

489

490 3.3.4.The application of HGMS to the Glensaugh farm sample demonstrated the effectiveness
491 of the method to extract MPs from soils. The higher recovery of MP particles and fibres
492 by HGMS from soil will enable researchers and practitioners in the agricultural and food
493 industries to understand the true impact of agricultural films and soil amendments on
494 soil quality and health. It has been reported that the consumption of macroplastics (> 5
495 mm) and MPs by sheep through grazing can occur (Beroit et al., 2021). MPs can also
496 affect crop growth and yield (Khalid et al., 2020) or have the potential to be incorporated

497 into crops, fruits or vegetables (Conti et al., 2020; Dong et al., 2021; Li et al., 2020).
498 Therefore, the developed HGMS method could potentially help with soil monitoring and
499 subsequently inform the agriculture and food industries.

500

501 **3.4. Evaluation of the HGMS method**

502 3.4.1.HGMS was a significantly faster method, taking ~30 min to process one sample,
503 compared to 2-3 days for DS. In this HGMS method, ethanol was used, which is readily
504 biodegradable and non-toxic (Thomas et al., 2020), whereas, DS uses salt solutions that
505 are toxic and have long lasting environmental effects (Thomas et al., 2020). Ethanol is
506 also substantially cheaper than the salts used in DS. Ethanol was used because it has a
507 low specific density, which resulted in better dispersion of lighter MPs into solution,
508 improving both settling times, and contact times with the collector wire during Stages 1
509 and 3. Water was considered during development of the HGMS method, but this caused
510 the flotation of lighter MPs and fibres preventing them from reaching the collector wire
511 within the electromagnetic field for high-gradient magnetic extraction in Stage 3 (data
512 not shown). Ethanol also has minimal impacts on MPs (Dawson et al., 2020).

513

514 3.4.2.This proof-of-concept study was intended to show the potential of HGMS to extract MPs
515 from soil. The HGMS system can be easily adapted by other researchers who wish to
516 build on this concept. Various filter designs are available commercially (or are easy to
517 make) to accommodate a range of separation requirements, from large to small sample
518 volumes to ones designed for specific sizes or quantities of target components or types
519 of matrices. Since HGMS works as a function of magnetic forces and magnetic
520 susceptibility and radius of the MP, a scaled-up system would simply require the
521 quantity of modified iron nanoparticles and the capacity/throughput of the HGMS set-

522 up to be adjusted appropriately. Larger HGMS systems have indeed been used in the
523 mining industry (Chun, 1995; Dahe, 2000; Ignjatović et al., 1995) and laboratory HGMS
524 systems of various sizes are available.

525

526 3.4.3. In summary, HGMS is a faster, safer and cheaper extraction method; it is also a mature
527 industrial technology (Alves et al., 2019; Gerber and Birss, 1983; Hillier and Hodson,
528 1997; Mullins, 1977; Rikers et al., 1998; Watson, 1973; Yavuz et al., 2009) that may be
529 further optimised for MP separation on a larger scale.

530

531 3.4.4. A potential drawback of the novel HGMS method is that some knowledge of the soil
532 composition and particle size may be required prior to MP extraction as this influences
533 the parameters required for separation. However, it is possible to identify broad soil
534 types relatively easily by hand texturing (Arshad et al., 1997). In this study, laser
535 diffraction particle size analysis and Dumas combustion procedures were carried out to
536 accurately determine soil particle size and carbon content, respectively. However, hand
537 texturing would allow these extra analysis steps to be by-passed. This proof-of-concept
538 work has already optimised HGMS conditions for four soil types (loam, high-carbon
539 loamy sand, sandy loam and high-clay sandy loam), and so it is likely that similar
540 experimental conditions can be used for similar soil types by other researchers wishing
541 to replicate this experimental set-up. Moreover, the conditions prescribed to the four
542 test soil types were used as a benchmark for assigning magnetic flux densities to the
543 Glensaugh farm sample, where the soil parameters differed to those in the test samples.
544 Therefore, optimising a particular soil sample for recovery is not a time-consuming task.
545 A further drawback is that some MPs may be lost during Stage 1. Any untreated MPs
546 adhered to the collector wire or physically trapped in the magnetic deposit that

547 accumulated on the wire in Stage 1 were discarded along with the magnetic soil
548 particles, which likely accounted for the losses observed. Despite this, the novel HGMS
549 method still out-performed the commonly used DS method and previous magnetic
550 extraction method (Grbic et al., 2019) with recoveries ranging between 87-100% for all
551 the MPs and fibres in this study.

552

553 **4. CONCLUSION**

554 4.1. The novel HGMS extraction method achieved high recoveries for both high- and low-density
555 MPs and fibres across a range of soil types. It is a fast and inexpensive method of extraction
556 avoiding the use of expensive and toxic chemicals as used by the DS method. This method
557 was also capable of recovering fibre-aggregate complexes enabling more accurate
558 enumeration of MP pollution in soils. Further work will be required to streamline the process
559 (e.g. calibrate the set up to accommodate more soil types, larger sample volumes and
560 optimise the design of the HGMS filter (collector wire)). However, even in a simple
561 configuration, such as that used in the present investigation, this improved extraction
562 method will provide an alternative quicker and more accurate method of quantifying and
563 monitoring MP contamination in environmental samples in future studies and would be
564 beneficial for the food, agricultural and environmental sectors.

565

566 **ACKNOWLEDGEMENTS**

567 This work was funded by the Macaulay Development Trust. EP, RH, LD and SH are supported by the
568 Scottish Government's Rural and Environmental Science and Analytical Services (RESAS) Division. SD
569 is supported by James Hutton Limited. The authors would like to thank Dr Allan Lilly and Pat Cooper
570 for providing test soils and the Glensaugh soil, respectively. They would also like to thank the James

571 Hutton Analytical Services for determination of soil chemistry, and Graham Gaskin for providing
572 support with the HGMS set-up.

573

574 **REFERENCES**

575 Alves MN, Miró M, Breadmore MC, Macka M. Trends in analytical separations of magnetic
576 (nano)particles. *Trends in Analytical Chemistry*. 2019; 114: 89-97. DOI:
577 <http://dx.doi.org/10.1016/j.trac.2019.02.026>

578 Arshad MA, Lowery B and Grossman B. Physical tests for monitoring soil quality. *Methods for assessing*
579 *soil quality*. 1997; 49, 123-141. DOI: <https://doi.org/10.2136/sssaspecpub49.c7>

580 Beriot N, Peek J, Zornoza R, Geissen V, Huerta Lwanga E. Low density-microplastics detected in sheep
581 faeces and soil: A case study from the intensive vegetable farming in Southeast Spain. *Science of The*
582 *Total Environment*. 2021; 755, 142653. DOI: <https://doi.org/10.1016/j.scitotenv.2020.142653>

583 Bhakdi SC, Ottinger A, Somsri S, Sratongno P, Pannadaporn P, Chimma P, Malasit P, Pattanapanyasat
584 K, Neumann HPH. Optimized high gradient magnetic separation for isolation of Plasmodium-infected
585 red blood cells. *Malaria Journal*. 2010; 9(38). DOI: <https://doi.org/10.1186/1475-2875-9-38>

586 Bläsing M & Amelung W. Plastics in soil: Analytical methods and possible sources. *Science of the Total*
587 *Environment*. 2018; 612, 422-435. DOI: <http://dx.doi.org/10.1016/j.scitotenv.2017.08.086>

588 British Standards Institution (2009) *BS EN ISO 13320:2009: Particle size analysis – Laser diffraction*
589 *methods*. Available at: <https://www.iso.org/standard/44929.html> (Accessed: 02 February 2021).

590 Chae Y & An Y-J. Current research trends on plastic pollution and ecological impacts on the soil
591 ecosystem: A review. *Environmental Pollution*. 2018; 240, 387-395. DOI:
592 <https://doi.org/10.1016/j.envpol.2018.05.008>

593 Chun YK. The removal of iron from hard pulverised kaolin by dry high-gradient magnetic separation.
594 *Magnetic and Electrical Separation*. 1995; 6, 171-177.

595 Claessens M, Van Cauwenberghe L, Vandeghuchte MB, Janssen CR. New techniques for the detection
596 of microplastics in sediments and field collected organisms. *Marine Pollution Bulletin*. 2013; 70, 227-
597 233. DOI: <http://dx.doi.org/10.1016/j.marpolbul.2013.03.009>

598 Conti GO, Ferrane M, Banni M, Favara C, Nicolosi I, Cristaldi A, Fiore M, Zuccarello P. Micro- and nano-
599 plastics in edible fruit and vegetables. The first diet risks assessment for the general population.
600 *Environmental Research*. 2020; 187, 109677. DOI: <https://doi.org/10.1016/j.envres.2020.109677>

601 Corradini F, Meza P, Eguiluz R, Casado F, Huerta-Lwanga E & Geissen V. Evidence of microplastic
602 accumulation in agricultural soils from sewage sludge disposal. *Science of the Total Environment*. 2019;
603 671, 411-420. DOI: <https://doi.org/10.1016/j.scitotenv.2019.03.368>

604 Dahe X. A large scale application of SLon magnetic separator in Meishan iron ore mine. *Magnetic and*
605 *Electrical Separation*. 2000; 11, 1-8. DOI: <https://doi.org/10.1080/10556910211967>

606 Dawson AL, Motti CA and Kroon FJ. Solving a Sticky Situation: Microplastic Analysis of Lipid-Rich Tissue.
607 *Frontiers in Environmental Science*. 2020; 8:563565. DOI: <https://doi.org/10.3389/fenvs.2020.563565>

608 de Souza Machado AA, Kloas W, Zarfl C, Hempel S, Rillig MC. Microplastics as an emerging threat to
609 terrestrial ecosystems. *Global Change Biology*. 2018a; 24, 1405-1416. DOI:
610 <https://doi.org/10.1111/gcb.14020>

611 de Souza Machado AA, Lau CW, Till J, Kloas W, Lehmann A, Becker R, Rillig MC. Impacts of Microplastics
612 on the Soil Biophysical Environment. *Environmental Science & Technology*. 2018b; 52, 9656-9665. DOI:
613 <https://doi.org/10.1021/acs.est.8b02212>

614 de Winter JCF. Using the Student's t-test with extremely small sample sizes. *Practical Assessment,*
615 *Research and Evaluation*. 2013; 18, Article 10. DOI: <https://doi.org/10.7275/e4r6-dj05>

616 Dong Y, Gao M, Qiu W, Song Z. Uptake of microplastics by carrots in presence of As (III): Combined
617 toxic effects. *Journal of Hazardous Materials*. 2021; 411, 125055. DOI:
618 <https://doi.org/10.1016/j.jhazmat.2021.125055>

619 Dris R, Gasperi J, Rocher V, Tassin B. Synthetic and non-synthetic anthropogenic fibers in a river
620 under the impact of Paris Megacity: Sampling methodological aspects and flux estimations. *Science*
621 *of the Total Environment*. 2018; 618, 157-164. DOI: <https://doi.org/10.1016/j.scitotenv.2017.11.009>

622 Ebner AD, Ritter JA, Nuñez L. High-gradient magnetic separation for the treatment of high-level
623 radioactive wastes. *Separation Science and Technology*. 1999; 34, 1333-1350. DOI:
624 <https://doi.org/10.1080/01496399908951096>

625 Enders K, Tagg AS, Labrenz M. Evaluation of Electrostatic Separation of Microplastics From Mineral-
626 Rich Environmental Samples. *Frontiers in Environmental Science*. 2020; 8, 122. DOI:
627 <https://doi.org/10.3389/fenvs.2020.00112>

628 Felsing S, Kochleus C, Buchinger S, Brennholt, Stock F, Reifferscheid G. A new approach in separating
629 microplastics from environmental samples based on their electrostatic behavior. *Environmental*
630 *Pollution*. 2018; 234, 20-28. DOI: <https://doi.org/10.1016/j.envpol.2017.11.013>

631 Gerber R, and Birss RR, 1983, High Gradient Magnetic Separation: Chichester, U.K., John Wiley and
632 Sons, 208 p.

633 Grause G, Kuniyasu Y, Chien M-F, Ilnoue C. Separation of microplastic from soil by centrifugation and
634 its application to agricultural soil. *Chemosphere*. 2022; 132654. DOI:
635 <https://doi.org/10.1016/j.chemosphere.2021.132654>

636 Grbic J, Nguyen B, Guo E, You JB, Sinton DL, Rochman CM. Magnetic Extraction of Microplastics from
637 Environmental Samples. *Environmental Science and Technology Letters*. 2019; 6: 68-72. DOI:
638 <https://doi.org/10.1021/acs.estlett.8b00671>

639 Gui J, Sun Y, Wang J, Chen X, Zhang S, Wu D. Microplastics in composting of rural domestic waste:
640 abundance, characteristics, and release from the surface of macroplastics. *Environmental Pollution*.
641 2021; 274, 116553. DOI: <https://doi.org/10.1016/j.envpol.2021.116553>

642 Guo J-J, Huang X-P, Xiang L, Wang Y-Z, Li Y-W, Li H, Cai Q-Y, MO c-h, Wong M-H. Source, migration
643 and toxicology of microplastics in soil. *Environmental International*. 2020; 137, 105263. DOI:
644 <https://doi.org/10.1016/j.envint.2019.105263>

645 Han X, Lu X & Vogt RD. An optimized density-based approach for extracting microplastics from soil and
646 sediment samples. *Environmental Pollution*. 2019; 254, 113009. DOI:
647 <https://doi.org/10.1016/j.envpol.2019.113009>

648 He D, Luo Y, Lu S, Liu M, Song Y, Lei L. Microplastics in soils: Analytical methods, pollution
649 characteristics and ecological risks. *Trends in Analytical Chemistry*. 2018; 109, 163-172. DOI:
650 <https://doi.org/10.1016/j.trac.2018.10.006>

651 Henry B, Laitala K & Klepp IG. Microfibres from apparel and home textiles: Prospects for including
652 microplastics in environmental sustainability assessment. *Science of the Total Environment*. 2019; 652,
653 483-494. DOI: <https://doi.org/10.1016/j.scitotenv.2018.10.166>

654 Hillier S, Hodson ME. High-gradient magnetic separation applied to sand-size particles: An example of
655 feldspar separation from mafic minerals. *Journal of Sedimentary Research*. 1997; 67: 975-977. DOI:
656 <http://dx.doi.org/10.2110/jsr.67.975>

657 Huerta Lwanga E, Gertsen H, Gooren H, Peters P, Salánki T, van der Ploeg M, Besseling E, Koelmans AA
658 and Geissen V. Microplastics in the Terrestrial Ecosystem: Implications for *Lumbricus terrestris*
659 (Oligochaeta, Lumbricidae). *Environmental Science and Technology*. 2016; 50, 2685-2691. DOI:
660 <https://doi.org/10.1021/acs.est.5b05478>

661 Hurly RR, Lusher AL, Olsen M, Nizzetto L. Validation of a Method for Extracting Microplastics from
662 Complex, Organic-Rich, Environmental Matrices. *Environmental Science & Technology*. 2018; 52, 7409-
663 7417. DOI: <https://doi.org/10.1021/acs.est.8b01517>

664 Ignjatović MR, Čalić N, Marković ZS, Ignjatović R. Development of a combined gravity-magnetic
665 separation process for magnetite ore using HGMS. *Magnetic and Electrical Separation*. 1995; 6, 161-
666 170.

667 Keyser PT and Jefferts SR. Magnetic susceptibility of some materials used for apparatus construction
668 (at 295 K). *Review of Scientific Instruments*. 1989; 60, 2711-2714. DOI:
669 <http://dx.doi.org/10.1063/1.1140646>

670 Khalid N, Aqeel M, Noman A. Microplastics could be a threat to plants in terrestrial systems directly
671 or indirectly. *Environmental Pollution*. 2020; 267, 115653. DOI:
672 <https://doi.org/10.1016/j.envpol.2020.115653>

673 Koelmans AA, Nor NHM, Hermesen E, Kooi M, Mintenig SM, De France J. Microplastics in freshwaters
674 and drinking water: Critical review and assessment of data quality. *Water Research*. 2019; 155, 410-
675 422. DOI: <https://doi.org/10.1016/j.watres.2019.02.054>

676 Li L, Luo Y, Li R, Zhou Q, Peijnenburg WJGM, Yin N, Yang J, Tu C, Zhang Y. Effective uptake of
677 submicrometre plastics by crop plants via a crack-entry mode. *Nature Sustainability*. 2020; 3, 929-937.
678 DOI: <https://doi.org/10.1038/s41893-020-0567-9>

679 Liu M, Lu S, Song Y, Lei L, Hu J, Lv W et al. Microplastic and mesoplastic pollution in farmland soils in
680 suburbs of Shanghai, China. *Environmental Pollution*. 2018; 242, 855-862. DOI:
681 <https://doi.org/10.1016/j.envpol.2018.07.051>

682 Liu M, Song Y, Lu S, Qiu R, Hu J, Li X, Bigalke M, Shi H, He D. A method for extracting soil microplastics
683 through circulation of sodium bromide solutions. *Science of the Total Environment*. 2019; 691, 341-
684 347. DOI: <https://doi.org/10.1016/j.scitotenv.2019.07.144>

685 Masura J, Baker J, Foster G, Arthur C, Herring C. 2015. Laboratory methods for the analysis of
686 microplastics in the marine environment: recommendations for quantifying synthetic particles in
687 waters and sediments. NOAA Technical Memorandum NOS-OR&R-48.

688 Mateos-Cárdenas A, van Pelt FNAM, O'Halloran J and Jansen MAK. Adsorption, uptake and toxicity of
689 micro- and nanoplastics: Effects on terrestrial plants and aquatic macrophytes. *Environmental*
690 *Pollution*. 2021; 284, 117183. DOI: <https://doi.org/10.1016/j.envpol.2021.117183>

691 Mullins CE. Magnetic Susceptibility of the Soil and its Significance in Soil Science – A Review. *Journal*
692 *of Soil Science*. 1977; 28(2), 223-246. DOI: <https://doi.org/10.1111/j.1365-2389.1977.tb02232.x>

693 Ng E, Huerta Lwanga E, Eldridge SM, Jonshton P, Hu H, Geissen V and Chen D. An overview of
694 microplastic and nanoplastic pollution in agroecosystems. *Science of the Total Environment*. 2018;
695 627, 1377-1388. DOI: <https://doi.org/10.1016/j.scitotenv.2018.01.341>

696 Pathan SI, Arfaioli P, Bardelli T, Ceccherini MT, Nannipieri P and Pietramellara G. Soil Pollution from
697 Micro- and Nanoplastic Debris: A Hidden and Unknown Biohazard. *Sustainability*. 2020; 12, 7255. DOI:
698 <https://doi.org/10.3390/su12187255>

699 Pella E and Colombo B. Study of carbon, hydrogen and nitrogen by combustion gas-chromatography.
700 *Mikrochim Acta*. 1973; 1973, 697-719. DOI: <https://doi.org/10.1007/BF01218130>

701 PlasticsEurope, 2019. Plastics – the Facts 2019. An Analysis of European Plastics Production, Demand
702 and Waste Data. Association of Plastics Manufactures, Brussels. Plastics Europe. Available online at:
703 <https://www.plasticseurope.org/en/resources/publications/1804-plastics-facts-2019> (Accessed 02
704 February 2021).

705 Prata JC, da Costa JP, Duarte AC, Rocha-Santos T. Methods for sampling and detection of microplastics
706 in water and sediment: A critical review. *Trends in Analytical Chemistry*. 2019a; 110, 150-159. DOI:
707 <https://doi.org/10.1016/j.trac.2018.10.029>

708 Prata JC, da Costa JP, Girão AV, Lopes I, Duarte AC, Rocha-Santos T. Identifying a quick and efficient
709 method of removing organic matter without damaging microplastic samples. *Science of the Total*
710 *Environment*. 2019b; 686, 131-139. DOI: <https://doi.org/10.1016/j.scitotenv.2019.05.456>

711 Prata JC, da Costa JP, Lopes I, Duarte AC, Rocha-Santos T. Environmental exposure to microplastics:
712 An overview on possible human health effects. *Science of the Total Environment*. 2020; 702, 134455.
713 DOI: <https://doi.org/10.1016/j.scitotenv.2019.134455>

714 Prendergast-Miller MT, Katsiamides A, Abbass M, Sturzenbaum SR, Thorpe KL, Hodson ME. Polyester-
715 derived microfibre impacts on the soil-dwelling earthworm *Lumbricus terrestris*. *Environmental*
716 *Pollution*. 2019; 251, 453-459. DOI: <https://doi.org/10.1016/j.envpol.2019.05.037>

717 Radford F, Zapata-Restrepo LM, Horton AA, Hudson MD, Shaw PJ, Williams ID. Developing a systematic
718 method for extraction of microplastics in soils. *Analytical Methods*. 2021; 13, 1695-1705. DOI:
719 <https://doi.org/10.1039/D0AY02086A>

720 Rikers RA, Rem P, Dalmijn WL & Honders A. Characterization of Heavy Metals in Soil by High Gradient
721 Magnetic Separation. *Journal of Soil Contamination*. 1998; 7(2): 163-190. DOI:
722 <https://doi.org/10.5402/2011/402647>

723 Rodríguez-Seijo A, da Costa JP, Rocha-Santos T, Duarte AC, Pereira R. Oxidative stress, energy
724 metabolism and molecular responses of earthworms (*Eisenia fetida*) exposed to low-density
725 polyethylene microplastics. *Environmental Science and Pollution Research*. 2018; 25, 33599-33610.
726 DOI: <https://doi.org/10.1007/s11356-018-3317-z>

727 Rolsky C, Kelkar V, Driver E, Halden RU. Municipal sewage sludge as a source of microplastics in the
728 environment. *Current Opinion in Environmental Science & Health*. 2020; 14, 16-22. DOI:
729 <https://doi.org/10.1016/j.coesh.2019.12.001>

730 Scheurer M & Bigalke M. Microplastics in Swiss Floodplain Soils. *Environmental Science & Technology*.
731 2018; 52, 3591-3598. DOI: <https://doi.org/10.1021/acs.est.7b06003>

732 Scopetani C, Chelazzi D, Mikola J, Leiniö V, Heikkinen R, Cincinelli A, Pellinen J. Olive oil-based method
733 for the extraction, quantification and identification of microplastics in soil and compost samples.
734 *Science of the Total Environment*. 2020; 733, 139338. DOI:
735 <https://doi.org/10.1016/j.scitotenv.2020.139338>

736 Shi X, Zhang X, Gao W, Zhang Y, He D. Removal of microplastics from water by magnetic nano-Fe₃O₄.
737 *Science of the Total Environment*. 2022; 802, 149838. DOI:
738 <https://doi.org/10.1016/j.scitotenv.2021.149838>

739 Sokolowska Z, Alekseev A, Skic K and Brzenzińska M. Impact of wastewater application on magnetic
740 susceptibility in Terric Histosol soil. *International Agrophysics*. 2016; 30, 89-94. DOI:
741 <https://doi.org/10.1515/intag-2015-0064>

742 Sthle L and Wold S. Analysis of variance (ANOVA). *Chemometrics and Intelligent Laboratory Systems*.
743 1989; 6, 259-272. DOI: [https://doi.org/10.1016/0169-7439\(89\)80095-4](https://doi.org/10.1016/0169-7439(89)80095-4)

744 Thomas D, Schütze B, Heinze WM and Steinmetz Z. Sample Preparation Techniques for the Analysis of
745 Microplastics in Soil—A Review. *Sustainability*. 2020; 12, 9074. DOI:
746 <https://doi.org/10.3390/su12219074>

747 Vithanage M, Ramanayaka S, Hasinthara S, Navaratne A. Compost as a carrier for microplastics and
748 plastic-bound toxic metals into agroecosystems. *Current Opinion in Environmental Science & Health*.
749 2021; 24, 100297. DOI: <https://doi.org/10.1016/j.coesh.2021.100297>

750 Wang Z, Taylor SE, Sharma P, Flury M. Poor extraction efficiencies of polystyrene nano- and
751 microplastics from biosolids and soil. *PLoS ONE*. 2018; 13, e0208009. DOI:
752 <https://doi.org/10.1371/journal.pone.0208009>

753 Watson JHP. Magnetic filtration. *Journal of Applied Physics*. 1973; 44, 4209-4213. DOI:
754 <https://doi.org/10.1063/1.1662920>

755 Welch BL. The Significance of the Difference Between Two Means when the Population Variances are
756 Unequal. *Biometrika*. 1938; 29, pp. 350–362. DOI: <https://doi.org/10.1093/biomet/29.3-4.350>

757 Yan Z, Liu Y, Zhang T, Zhang F, Ren H, Zhang Y. Analysis of Microplastics in Human Feces Reveals a
758 Correlation between Fecal Microplastics and Inflammatory Bowel Disease Status. *Environmental*
759 *Science and Technology*. 2022; 56, 414-421. DOI: <https://doi.org/10.1021/acs.est.1c03924>

760 Yavuz CT, Mayo JT, Yu WW, Prakash A, Falkner JC, Yean S, Cong L, Shipley HJ, Kan A, Tomson M,
761 Natelson D, Colvin VL. Low-Field Magnetic Separation of Monodisperse Fe₃O₄ Nanocrystals. *Science*.
762 2006; 314, 964-967. DOI: <https://doi.org/10.1126/science.1131475>

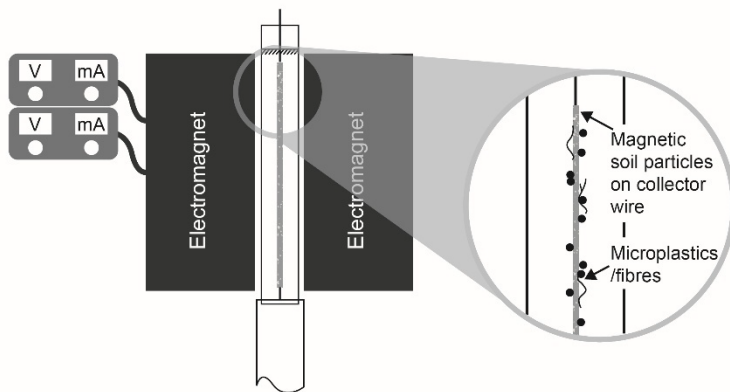
763 Yavuz CT, Prakash A, Mayo JT, Colvin VL. Magnetic separations: From steel plants to biotechnology.
764 *Chemical Engineering Science*. 2009; 64, 2510-2521. DOI: <https://doi.org/10.1016/J.CES.2008.11.018>

765 Zhang GS & Liu TF. The distribution of microplastics in soil aggregate fractions in southwestern China.
766 *Science of the Total Environment*. 2018; 642, 12-20. DOI:
767 <https://doi.org/10.1016/j.scitotenv.2018.06.004>

768 Zhang S, Wang J, Liu X, Qu F, Wang X, Wang X et al. Microplastics in the environment: A review of
769 analytical methods, distribution, and biological effects. *Trends in Analytical Chemistry*. 2019; 111: 62-
770 72. DOI: <https://doi.org/10.1016/j.trac.2018.12.002>

771 Zhang S, Yang X, Gertsen H, Peters P, Salánki T, Geissen V. A simple method for the extraction and
772 identification of light density microplastics from soil. *Science of the Total Environment*. 2018; 616-
773 617, 1056-1065. DOI: <https://doi.org/10.1016/j.scitotenv.2017.10.213>

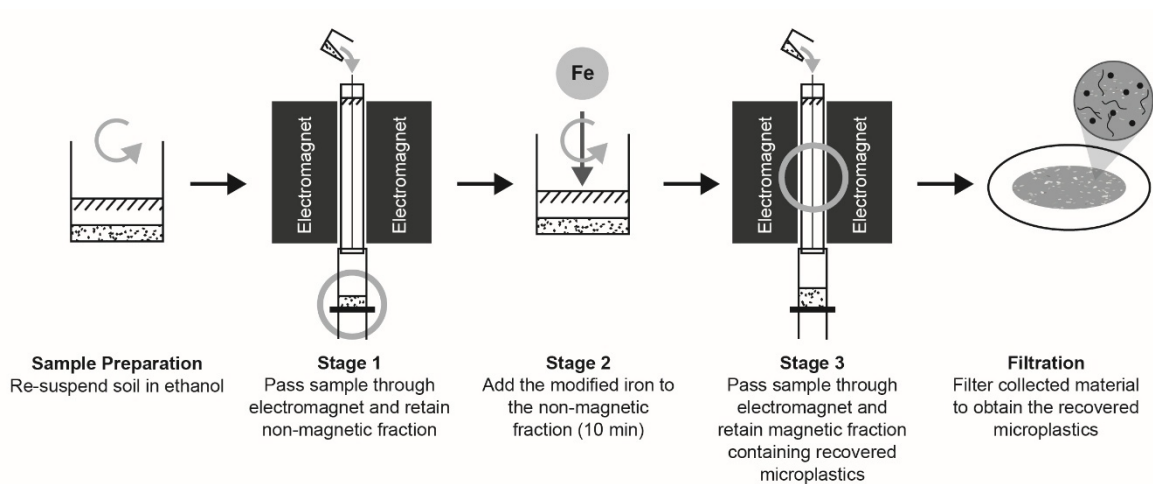
774



776

777 **Figure 1.** Schematic of the HGMS system showing the current suppliers, the electromagnet poles and
778 column containing the collector wire and ethanol where there are MPs adhered to the wire.

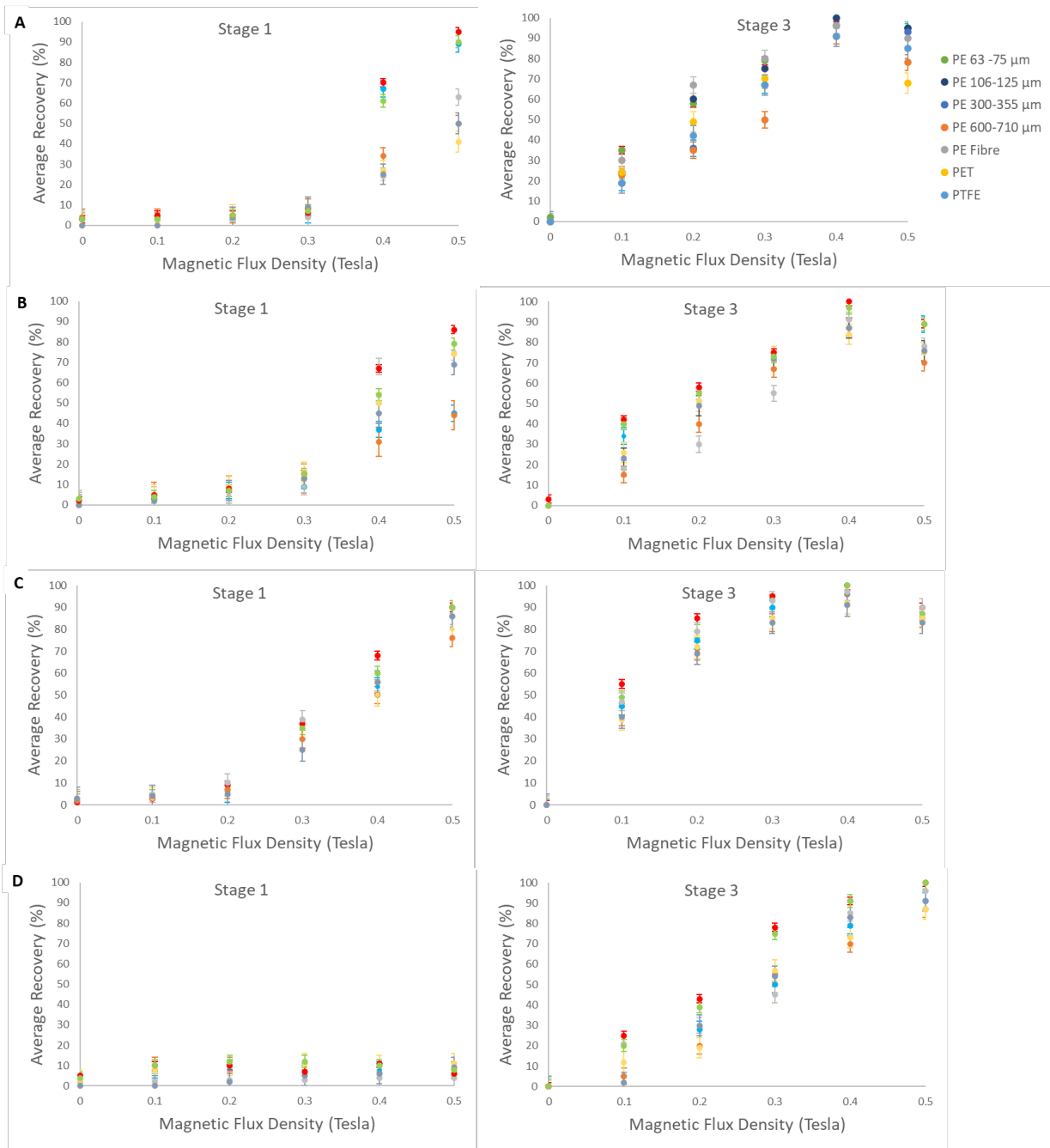
779



780

781 **Figure 2.** Schematic of the three-staged HGMS method.

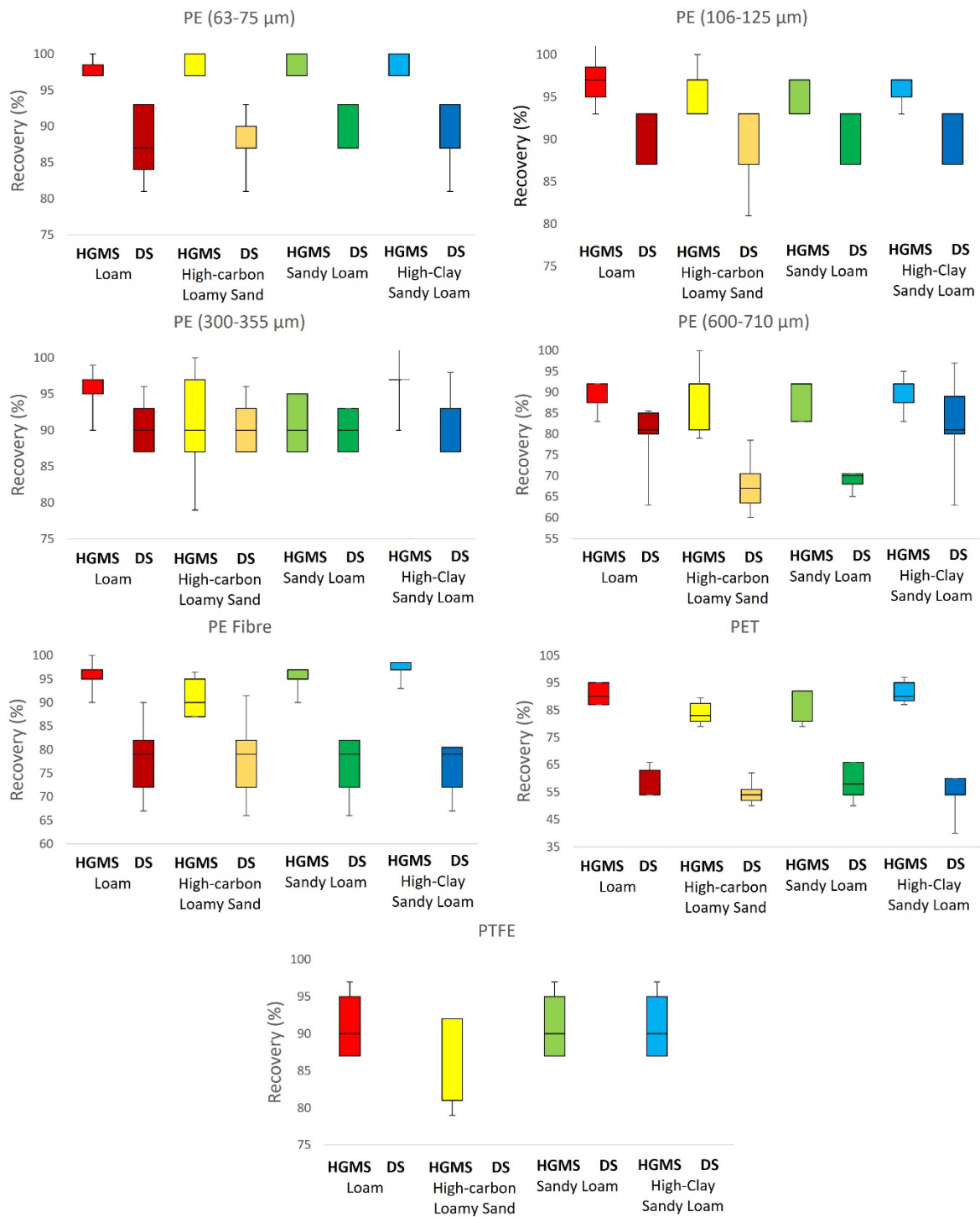
782



783

784 **Figure 3.** Influence of magnetic flux density on average MP recovery in (A) loam, (B) high-carbon loamy
 785 sand, (C) high-clay sandy loam, and (D) sandy loam for Stage 1 and Stage 3 of HGMS. Error bars indicate
 786 standard deviation.

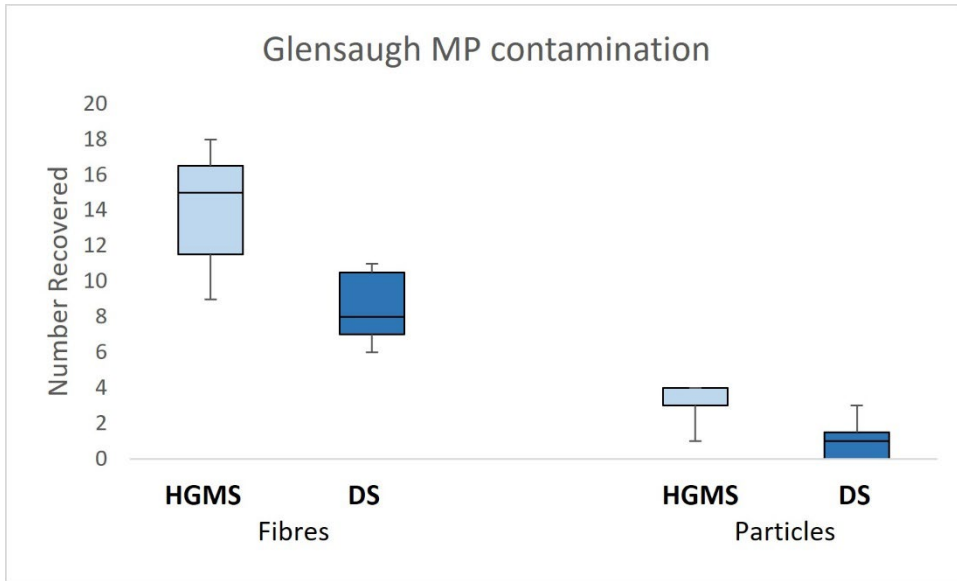
787



788

789 **Figure 4.** Box plots showing MP recovery using HGMS in each soil type (loam, high-carbon loamy sand,
 790 sandy loam and high-clay sandy loam) compared to DS. Colours indicate soil type. Errors bars show
 791 standard deviation.

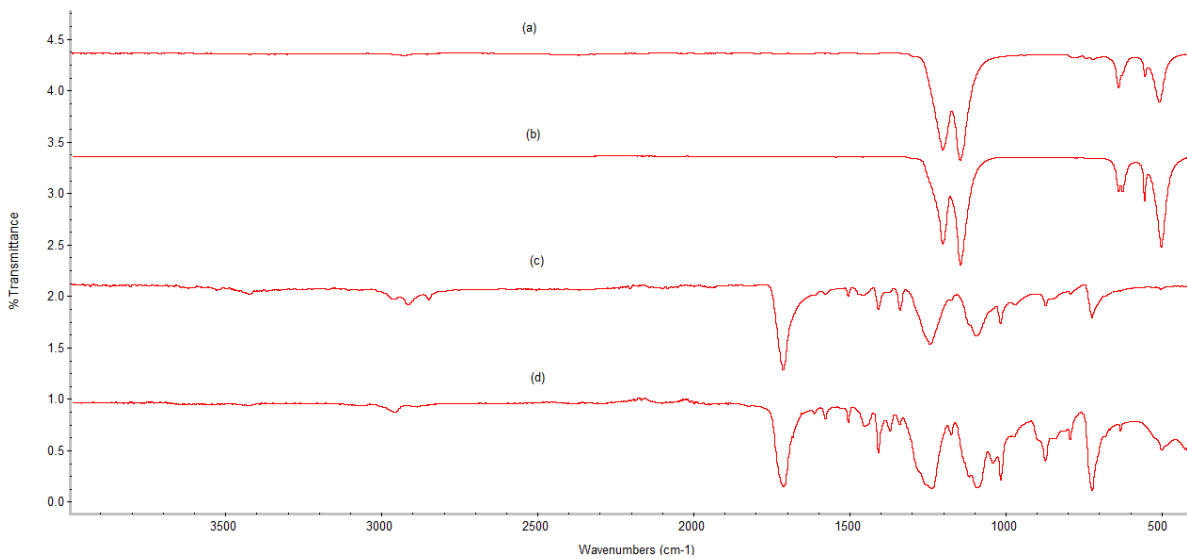
792



793

794 **Figure 5.** Box plot comparing the recovery of MP particles and fibres from the Glensaugh soil sample
 795 by HGMS and DS. Error bars depict standard deviation.

796



797

798 **Figure 6.** FTIR spectra of (a) a PTFE particle, and (c) a PET-glycol fibre recovered from the Glensaugh
 799 sample. Spectra (b) and (d) are their respective reference spectra.

800

801

802 **Table 1.** Soil Chemistry. Particle size ranges for clay, silt and sand, respectively, are indicated in the
 803 brackets.

Soil Type	Clay Content (%) (<2 µm)	Silt Content (%) (2-20 µm)	Sand Content (%) (20-2000 µm)	Carbon Content (%)	pH (in water)
Loam	10.07	43.17	46.76	3.00	5.17
High-Carbon	1.05	13.94	85.01	14.40	5.36
Loamy Sand					
Sandy Loam	4.98	21.55	73.47	2.33	5.08
High-Clay	21.00	20.00	59.00	4.79	5.45
Sandy Loam					
Glensaugh (sandy loam)	3.40	37.82	58.78	7.36	5.73

804

805 **Highlights**

- 806 • Rapid High-Gradient Magnetic Separation method for microplastic extraction from soil
- 807 • The HGMS method performed significantly better than the density separation method
- 808 • It was able to recover high- and low-density microplastics
- 809 • Could recover microplastic particles and fibres 63 µm – 15 mm in size (≥ 87%)
- 810 • Avoided the use and disposal of hazardous salts associated with density separation

811

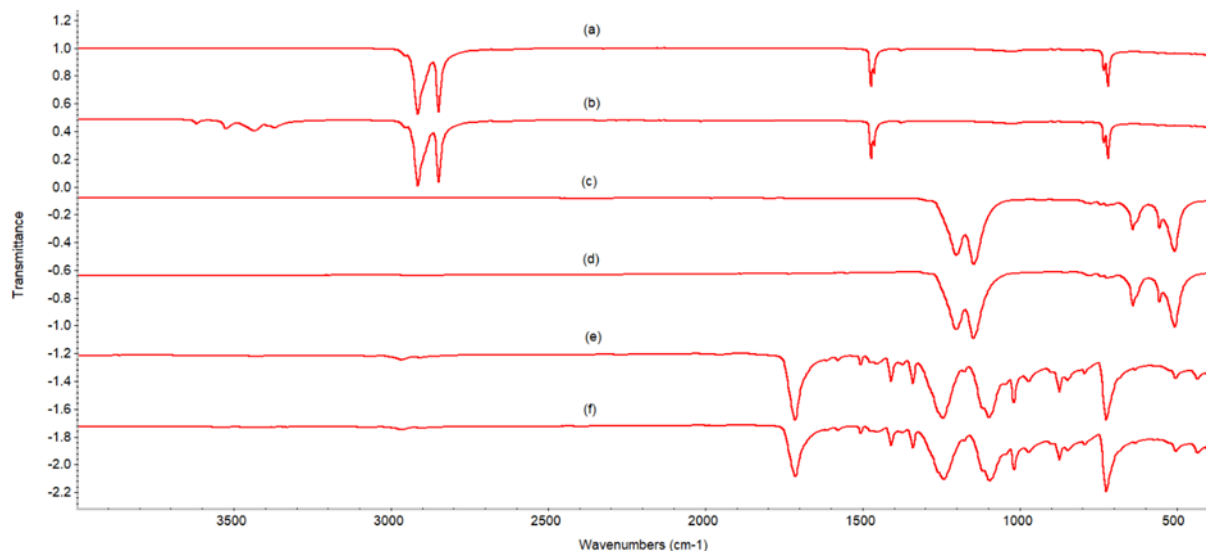
812 **Supplementary Material**



813

814 **Figure S1.** Photograph of a red fibre (identified predominantly as polyester by FTIR) partially
815 embedded in a soil aggregate under the stereomicroscope recovered from the Glensaugh
816 sample using the developed HGMS method.

817



818

819 **Figure S2.** Comparison of FTIR spectra of pristine (a) PE, (c) PTFE, and (e) PET particles to
820 modified iron-bound (b) PE, (d) PTFE, and (f) PET particles recovered from a test soil. The PE MPs
821 used here contained aluminium trihydrate (gibbsite) (troughs around 3500 cm⁻¹ region) – a
822 common plastic flame retardant filler (Shah et al., 2014).

823

824 **REFERENCES**

825 Shah AUR, Lee D, Wang Y, Wasy A, Ham KC, Jayaraman K, Kim B, Song J. Effect of concentration
826 of ATH on mechanical properties of polypropylene/aluminium trihydrate (PP/ATH) composite.
827 *Trans. Nonferrous Met. Soc. China.* 2014; 24, s81-s89. DOI: [https://doi.org/10.1016/S1003-](https://doi.org/10.1016/S1003-6326(14)63292-1)
828 [6326\(14\)63292-1](https://doi.org/10.1016/S1003-6326(14)63292-1)

829